On the morphology of poly(vinylidene fluoride) crystals in blends

D. Braun, M. Jacobs and G. P. Hellmann*
Deutsches Kunststoff-Institut, Schlossgartenstrasse 6, D-6100 Darmstadt, Germany
(Received 22 December 1992; revised 28 June 1993)

The crystallization of poly(vinylidene fluoride) (PVF_2) in homogeneous blends with poly(methyl methacrylate) (PMMA), a copolymer of styrene and MMA (PSMMA) or poly(methyl acrylate) (PMA) was investigated to establish the conditions leading to dendritic crystals. These unusual crystals feature branches, from which grow twigs, so that a tree-like, i.e. dendritic, structure results. In blends with PMMA or PSMMA, but not in blends with PMA, the α modification of PVF_2 forms such dendrites, while the γ modification forms more or less perfect spherulites. The dendritic crystals appear at moderate undercoolings, up to surprisingly high PVF_2 concentrations. The various spherulitic and dendritic structures observed in the blends can be explained in terms of a competition of crystallization and diffusion that produces concentration gradients in the melt.

(Keywords: poly(vinylidene fluoride); crystallization; blends)

INTRODUCTION

Crystalline poly(vinylidene fluoride) (PVF_2) has been studied frequently, in the bulk[1-10] as well as in blends[11-18], because it forms several modifications. This paper deals with the crystallization in isotropic melts. Pure PVF_2 is addressed, but most attention is given to its blends with poly(methyl methacrylate) (PMMA)[11-15], a random copolymer of styrene and MMA ($P(S_{0.13}MMA_{0.87})$)[16] or poly(methyl acrylate) (PMA)[17,18].

In the isotropic melt, PVF_2 forms α, γ and γ' crystals that melt in this order (*Figure 1a*). Primary nucleation leads either only to α ($T \leqslant 150°C$), or to α and γ, or only to γ crystals ($T \geqslant 170°C$)[1-10]. The γ' modification is formed in a secondary process, inside the α crystals, via a solid–solid transition[1,19]. *Figure 1b* shows a melting sequence, where first α disappears and then γ, leaving at the highest temperature only γ'. (The nomenclature is that of Morra and Stein[11]. The γ' modification crystallizes with the same unit cell as the γ modification.)

When α and γ are formed together in pure PVF_2, both grow as spherulites, as is shown in *Figure 2*. The only differences are that the α spherulites are often fibrillated and are usually larger. In blends, the differences in morphology can be much more drastic. *Figure 3* shows (i) small γ crystals that are imperfect *spherulites*, internally not much structured, and (ii) large α crystals that are perfect *dendrites*, with a complex internal structure of branches and twigs reminiscent of fractals[20,21].

This study was undertaken to determine the conditions for dendritic crystallization in various blends of PVF_2. An explanation for potentially dendritic growth of crystals in blends is illustrated by *Figure 4*. If a crystal grows into its own melt, fluctuations in its front are levelled off (*Figure 4a*), the driving force being minimization of the crystal–melt interface. On average, the crystal front will advance evenly, leading to a *spherulite*. But if the crystal grows in a homogeneous blend with an amorphous polymer, it can produce, at its front, a 'depletion layer' with less than average of the crystallizing chains ($w < \bar{w}$, *Figure 4b*). The maxima of the fluctuations stick out into this layer and are preferentially supplied by the melt ($w = \bar{w}$) with crystallizing chains. Therefore, the maxima grow further and can turn into long branches that leave depletion zones ($w < \bar{w}$) between them[22]. The branches can later branch again, which leads to the peculiar branch-and-twig structure of a *dendrite*†.

Dendrites are expected, according to Keith and Padden[22], if chain diffusion in the melt is relatively slow. Simulations yield particularly well developed dendrites if the crystallization is even diffusion-controlled[20]. Therefore, diffusion rates were varied, in the blends, by varying: the concentration of PVF_2; the glass transition temperature and the molecular weight of the amorphous polymer; as well as the interactions between PVF_2 and the amorphous polymer.

The composition of blends will be characterized by the weight fraction w of PVF_2.

EXPERIMENTAL

The PVF_2 was Solef 1008 from Solvay ($M_w = 100 \times 10^3$, $M_w/M_n = 2.5$). It had 4 mol% of head-to-head linkages.

† There are different opinions concerning the terms 'spherulite' and 'dendrite'. All crystals in *Figure 3* could be considered spherulites, because all are more or less spherical, but, on the other hand, all could be considered dendrites, because all grow branches from one centre. In this paper, compact 'normal' crystals such as those of the γ modification in *Figure 3* will be called 'spherulites', and loosely packed 'anomalous' crystals with extensive branching such as those of the α modification in *Figure 3* will be called 'dendrites', meaning 'tree-like'

* To whom correspondence should be addressed

0032-3861/94/04/0706-12

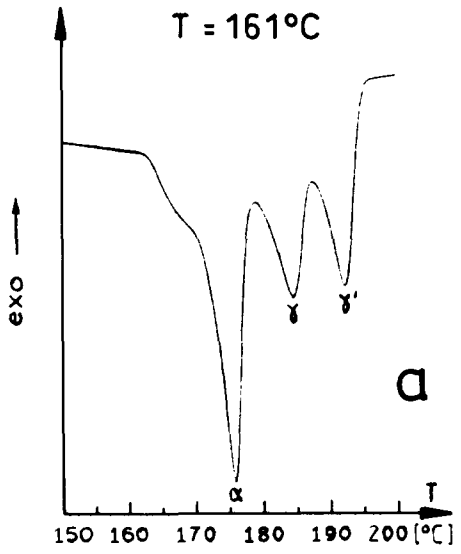

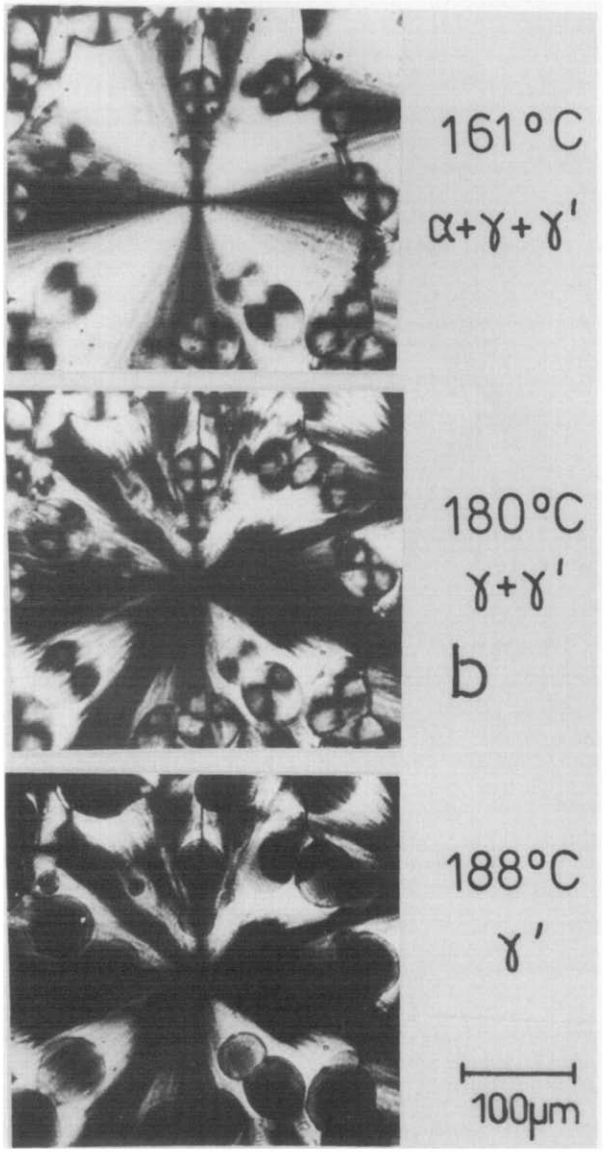

Figure 1 Melting of PVF_2 crystallized for 2 days at 161°C: (a) d.s.c. trace; (b) morphology with a large α crystal and small γ crystals, of which α melted below 180°C and γ below 188°C, revealing that sectors of the α crystal were already converted into γ'

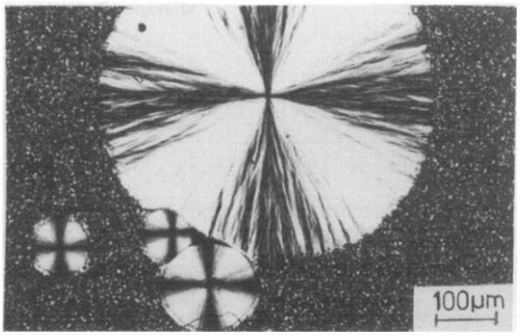

Figure 2 A large α and three small γ spherulites in PVF_2 (166°C)

The influence of these linkages has been investigated by Lovinger[1]. The PMMA was 8N from Röhm GmbH ($M_w = 97 \times 10^3$, $M_w/M_n = 2.1$). The copolymers of styrene and MMA (x = mole fraction of styrene) were made via radical polymerization to low conversion at 60°C, using azobisisobutyronitrile (AIBN) as the initiator ($M_w \simeq 170 \times 10^3$, $M_w/M_n \simeq 1.8$; copolymer $P(S_{0.13}MMA_{0.87})$: $M_w = 174 \times 10^3$, $M_w/M_n = 1.6$). Blends were prepared by slow film casting from γ-butyrolactone solution at 120°C under nitrogen. The films, 20–40 μm thick, were amorphous or crystalline with extremely small crystals. They were heated for 30 min to 200°C, in the d.s.c. or in an aluminium block oven, and then quenched to the crystallization temperature. Isothermal crystallization took place in the d.s.c., the block oven, or in a hot stage under the light microscope (Orthoplan, Leitz). Phase separation was determined microscopically, at a heating rate of 1 K min^{-1}. Glass transition temperatures were measured by d.s.c. (912, DuPont), 10 K min^{-1}.

RESULTS

Blends of PVF_2 and PMMA[12,18,23] or PMA[17,18] are homogeneous at all temperatures where the polymers are stable. The blend PVF_2/PMMA becomes immiscible above the (extrapolated) critical temperature $LCST \simeq 350$°C[18]. The $LCST$ of blends $PVF_2/P(S_xMMA_{1-x})$ decreases with increasing styrene content x as shown in *Figure 5*. Blends with $x \geqslant 0.15$ are immiscible at all temperatures.

The crystallization in homogeneous blends of PVF_2 with PMMA, $P(S_{0.13}MMA_{0.87})$ and PMA was studied in the temperature range 140–170°C, which is between the glass transition temperatures T_g and the melting points T_α^∞ (of the α modification, extrapolated in the Hoffman–Weeks fashion to infinitely slow crystallization[24]) shown in *Figure 6*. The T_g curves indicate that, in the temperature range in question, chain diffusion is fast for blends with PMA and much slower for those with PMMA and $P(S_{0.13}MMA_{0.87})$.

The particular copolymer ($P(S_{0.13}MMA_{0.87})$, from now on referred to simply as PSMMA, was chosen because its blend with PVF_2 is close to immiscibility (*Figure 5*), in contrast with PMMA, which has good interactions with PVF_2.

Blends with PMMA or PSMMA

The crystallization kinetics are treated first, then the morphologies are shown. Finally, the morphologies and the radial growth rates of the crystals are correlated.

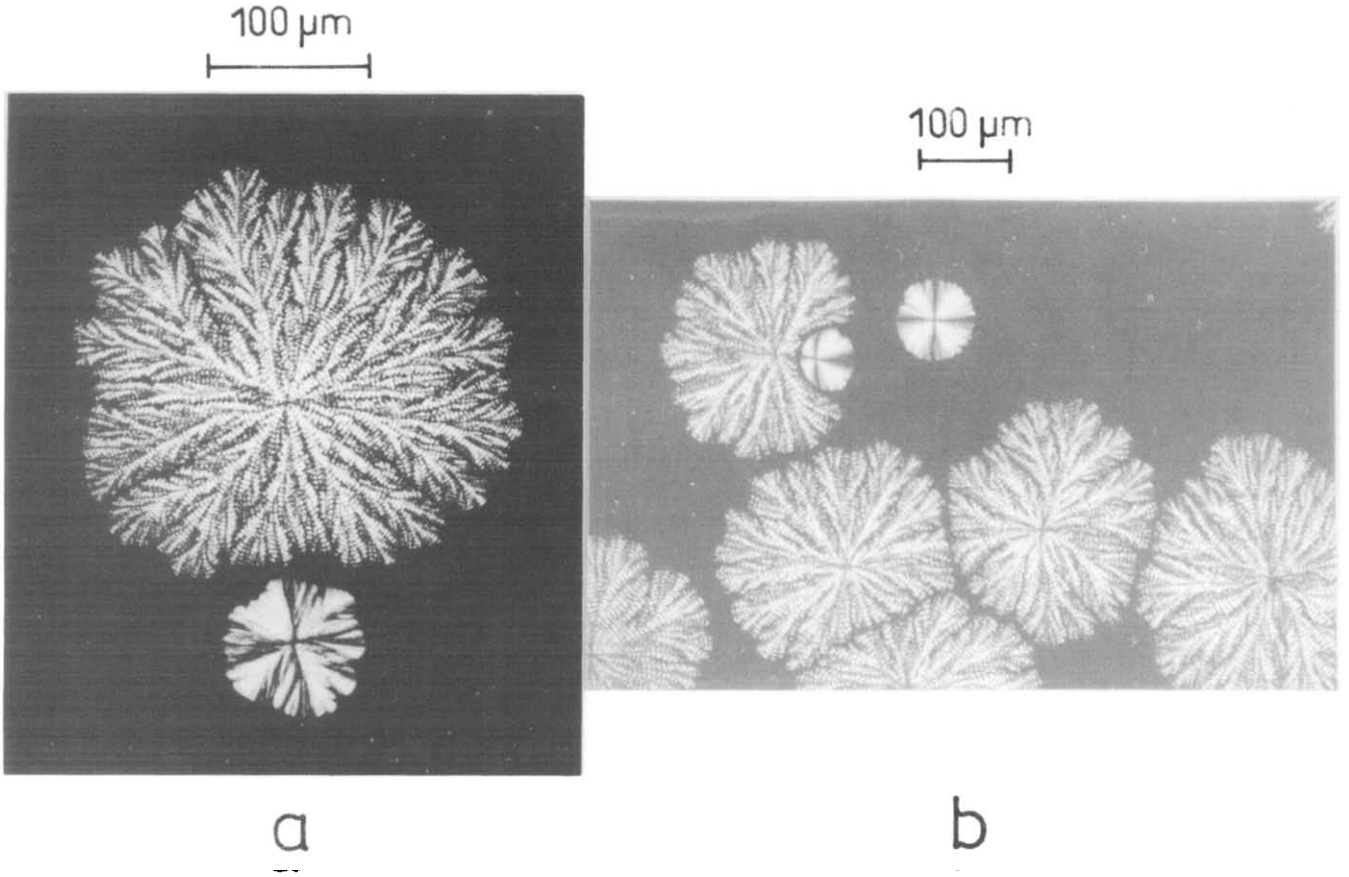

Figure 3 Large α dendrites and small γ spherulites in blends $PVF_2/P(S_{0.13}MMA_{0.87})$: (a) $w=0.6$ (160°C), (b) $w=0.4$ (155°C)

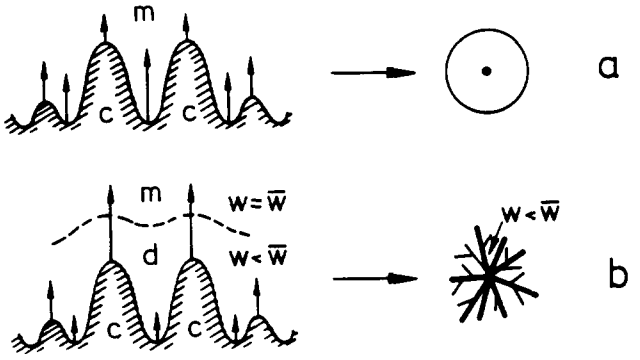

Figure 4 Fluctuations in the front of a crystal ('c') growing into the melt ('m'), arrows indicating the growth rate: (a) spherulitic and (b) dendritic growth. The concentration of crystallizable chains is $\bar{w}$ in the melt and $w<\bar{w}$ in the depletion layer ('d') below the broken line in (b)

Crystallization kinetics. The degree of crystallization of the α modification:

$$\xi_\alpha(t)=\Delta h_\alpha(t)/\Delta h_\alpha(t\rightarrow\infty) \qquad (1)$$

was determined using two d.s.c. methods (Δh = melting endotherm):

(i) At higher temperatures, where crystallization is slow, samples were annealed isothermally for times t and quenched. Then a d.s.c. trace $c_p(T)$ was measured. *Figure 7a* shows how the crystallinity of α, γ and γ′ develops. All γ′ was originally α. Therefore, the peaks α and γ′ were used together for $\Delta h_\alpha(t)$.

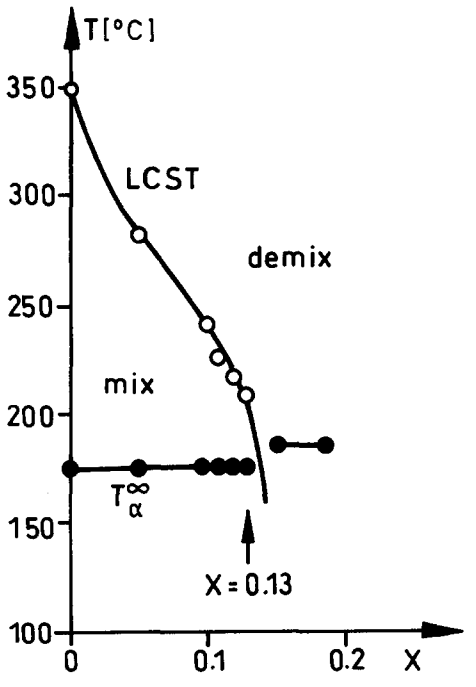

Figure 5 Critical temperature *LCST* of blends $PVF_2/P(S_xMMA_{1-x})$ and melting point T_α^∞ of the α modification

(ii) At lower temperatures, where crystallization is fast and only the α modification is formed, isothermal d.s.c. traces $c_p(t)$ were measured, on-line (*Figure 7b*), and the endotherm was directly integrated for $\Delta h_\alpha(t)$.

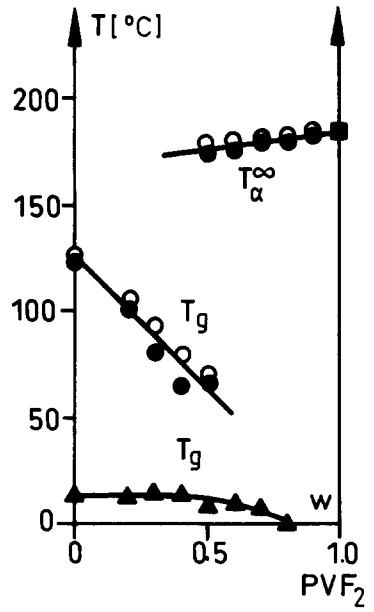

Figure 6 Melting points T_α^∞ and glass transition temperatures T_g of blends of PVF_2 with PMMA (●), PSMMA (○) and PMA (▲)

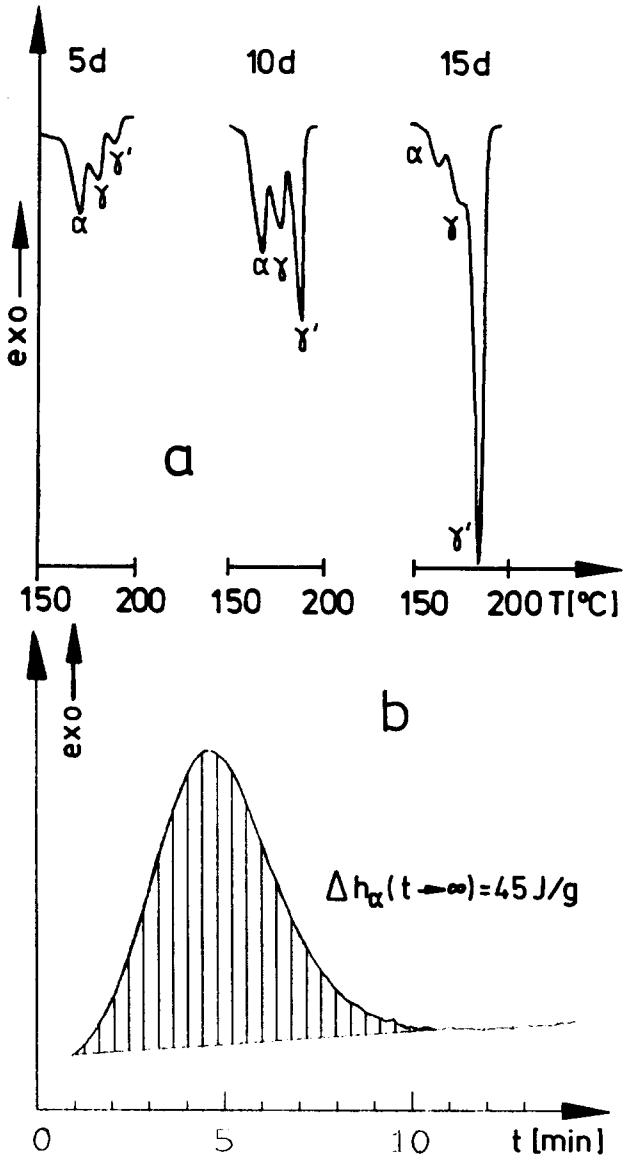

Figure 7 D.s.c. traces of blends $PVF_2/PMMA_{w=0.5}$: (a) $c_p(T)$ after crystallization for different times at 155°C; (b) $c_p(t)$ during crystallization at 110°C

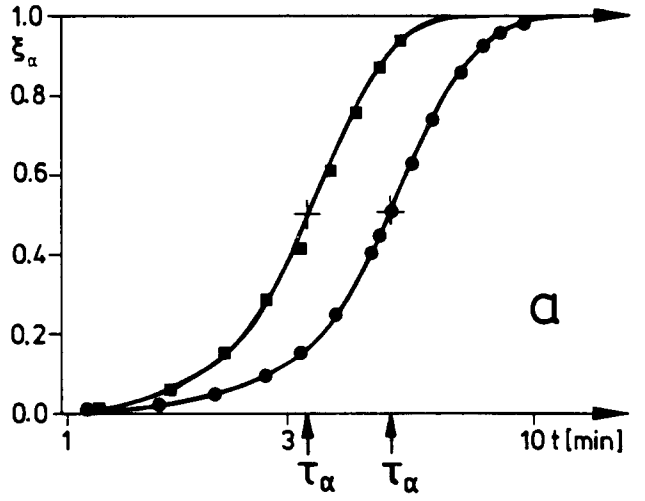

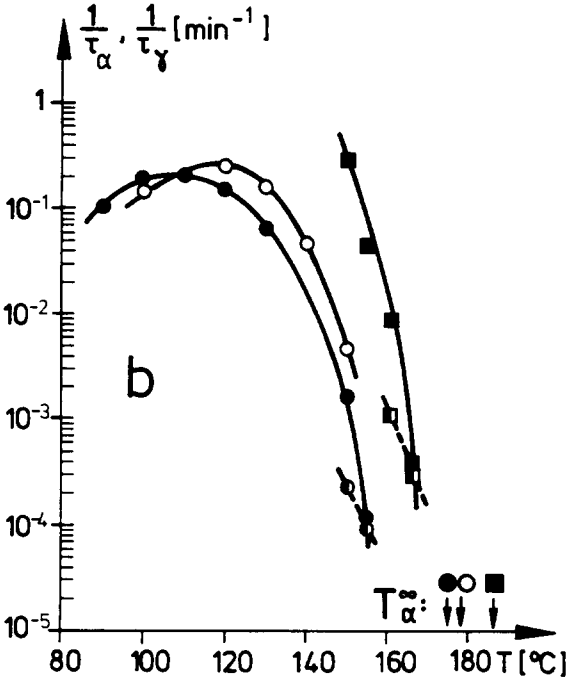

Figure 8 (a) Degree of α crystallization $\xi_\alpha(t)$ (equation (1)) of PVF_2 at 150°C (■) and of $PVF_2/PMMA_{w=0.5}$ at 110°C (●); (b) crystallization rates $1/\tau_\alpha(T)$ of PVF_2 (■) and $PVF_2/PMMA_{w=0.5}$ (●) (also shown by half-filled symbols are $1/\tau_\gamma$) and $1/\tau_\alpha(T)$ of $PVF_2/PSMMA_{w=0.5}$ (○). T_α^∞ = melting points at infinitely slow crystallization

The curves $\xi_\alpha(t)$ are of the Avrami type. The two curves in *Figure 8a* for pure PVF_2 and the blend $PVF_2/PMMA_{w=0.5}$ give an impression of how much slower crystallization is in the blends. The blend had to be undercooled by 40 K more than PVF_2, to arrive at a comparable crystallization rate.

The time τ_α of half-crystallization or, rather, $1/\tau_\alpha$ shown in *Figure 8b*, is a measure of the crystallization rate of the α modification. The curves $1/\tau_\alpha(T)$ have the convex shape predicted by the Hoffman–Lauritzen model[25,26]. The temperature of maximum crystallization rate is approximately 120°C. In what follows, crystallization is considered far above 120°C. Crystallization is always controlled primarily by the formation and growth rates of the crystal nuclei, not by the mobility in the amorphous matrix. Nevertheless, diffusion at crystal fronts will account for spectacular effects.

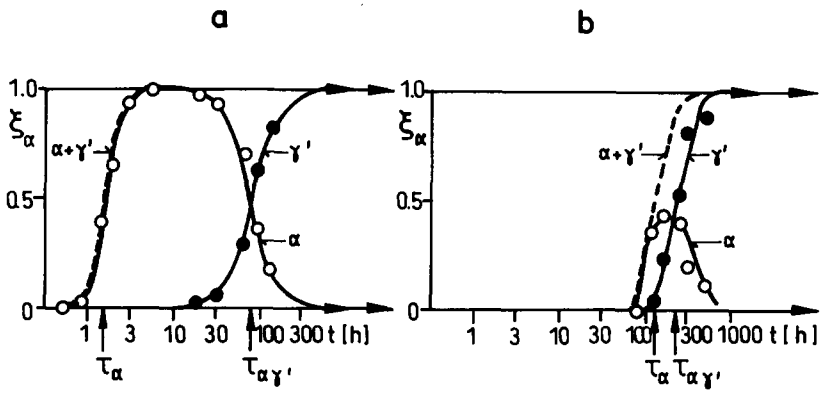

Figure 9 Degree of crystallization of the α (○), the γ' (●) and the combined (α + γ') crystallization (---) of (a) PVF_2 at 161°C and (b) PVF_2/PMMA$_{w=0.5}$ at 155°C. $\tau_{\alpha\gamma'}$ = characteristic time, where the conversion $\alpha \rightarrow \gamma'$ has arrived at $\xi_{\gamma'} = 0.5$

The γ modification takes over at high temperatures, close to the melting points. The rates $1/\tau_\gamma$ in *Figure 8b* were estimated from the volume fraction of γ crystals in micrographs after complete crystallization.

While τ_α and τ_γ respond to the high viscosity in the blends, and therefore depend strongly on temperature, the formation of the γ' modification[1,19] does not. *Figure 9* shows how ξ_α, which combines the α and γ' crystallinity, is composed of α and γ'. In PVF_2 (*Figure 9a*), all crystals that are born as α remain α, up to complete crystallization. They are converted into γ' only later, after the time lapse $(\tau_{\alpha\gamma'} - \tau_\alpha) \approx 10^2$ h. In the blend PVF_2/PMMA$_{w=0.5}$ (*Figure 9b*), however, the $\alpha \rightarrow \gamma'$ conversion proceeds already during α crystallization. But the time lag $(\tau_{\alpha\gamma'} - \tau_\alpha)$ is similar, meaning that γ' is indeed formed in a solid–solid conversion $\alpha \rightarrow \gamma'$. This process does not change the morphology at all. The formation of γ' is, therefore, irrelevant for the next sections.

Morphologies. The morphologies of the α modification were investigated in a window limited by (i) too rapid primary nucleation at $T < 140$°C, (ii) the transition to the γ modification at $T \geqslant 170$°C, and (iii) too slow crystallization at $w < 0.2$. *Figure 10* displays the distribution of three different morphologies of the α crystals. The two diagrams are similar. The different compatibility of PVF_2 with the amorphous polymer, PMMA or PSMMA, does not matter much.

The α morphologies distinguished in *Figure 10* are shown in *Figure 11*, in a series of blends crystallized at 160°C. Pure PVF_2 forms spherulites 'α_S'. These turn, at decreasing w, into dendrites 'α_D', which turn, at still lower w, into ringed spherulites 'α_{rS}'. The dominant features are radial fibrils (α_S), branches and twigs (α_D), and concentric rings (α_{rS}).

The categories α_S, α_{rS} and α_D are descriptive, but not exact. In particular, not only the α_{rS} spherulites but all types of α crystals exhibit a concentric ring pattern (difficult to see in α_S). The ring spacing d_{ring} increases with decreasing w (*Figure 12*). The rings are, therefore, most pronounced in the α_{rS} crystals. Such ring patterns have been observed in spherulites of pure polymers, too. They result from helical twisting of the optical axis in the crystals[11,27,28]. The rings thus do not indicate a primarily blend-specific effect. The spherulites α_S and α_{rS} are not different in a basic fashion.

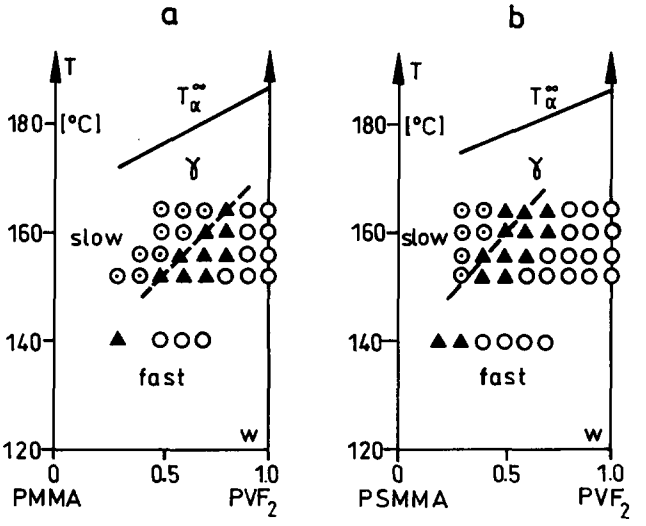

Figure 10 Types of morphology of the α modification in (a) PVF_2/PMMA and (b) PVF_2/PSMMA: α_S (○), α_D (▲), α_{rS} (⊙). T_α^∞ = melting points. Radial growth of the crystals is linear below and non-linear above the broken line (see *Figure 17*)

The peculiar changes of morphology observed in *Figure 11* with decreasing w, i.e. $\alpha_S \rightarrow \alpha_D \rightarrow \alpha_{rS}$, constitute, therefore, a double transition not between three types of structure, but between two types only. But this is even more puzzling: dilution of PVF_2 causes a change from spherulites to dendrites and back to spherulites!

The phase diagrams of *Figure 10* show spherulites α_S at high w, of course. But of interest is the range of lower w. The dendrites α_D appear in a sloped area that extends up to surprisingly high w, especially in the blends PVF_2/PMMA. The sequence $\alpha_S \rightarrow \alpha_D \rightarrow \alpha_{rS}$ is observed in the direction northwest. It can be obtained by lowering w or by raising the temperature.

The transitions $\alpha_S \rightarrow \alpha_D$ and $\alpha_D \rightarrow \alpha_{rS}$ are gradual. *Figure 13a* is an example for $\alpha_S \rightarrow \alpha_D$, and the dendrite in *Figure 11e* is an example for $\alpha_D \rightarrow \alpha_{rS}$. The latter is more compact, more related to the ringed spherulites α_{rS} in *Figure 11f*, than the dendrite in *Figure 3*, which is an early stage of *Figure 11d*.

After melting, the structure of dendrites α_D persists for a while (*Figure 13*), which cannot be seen under crossed (*Figure 13b*) but under parallel polars (*Figure 13c*). The

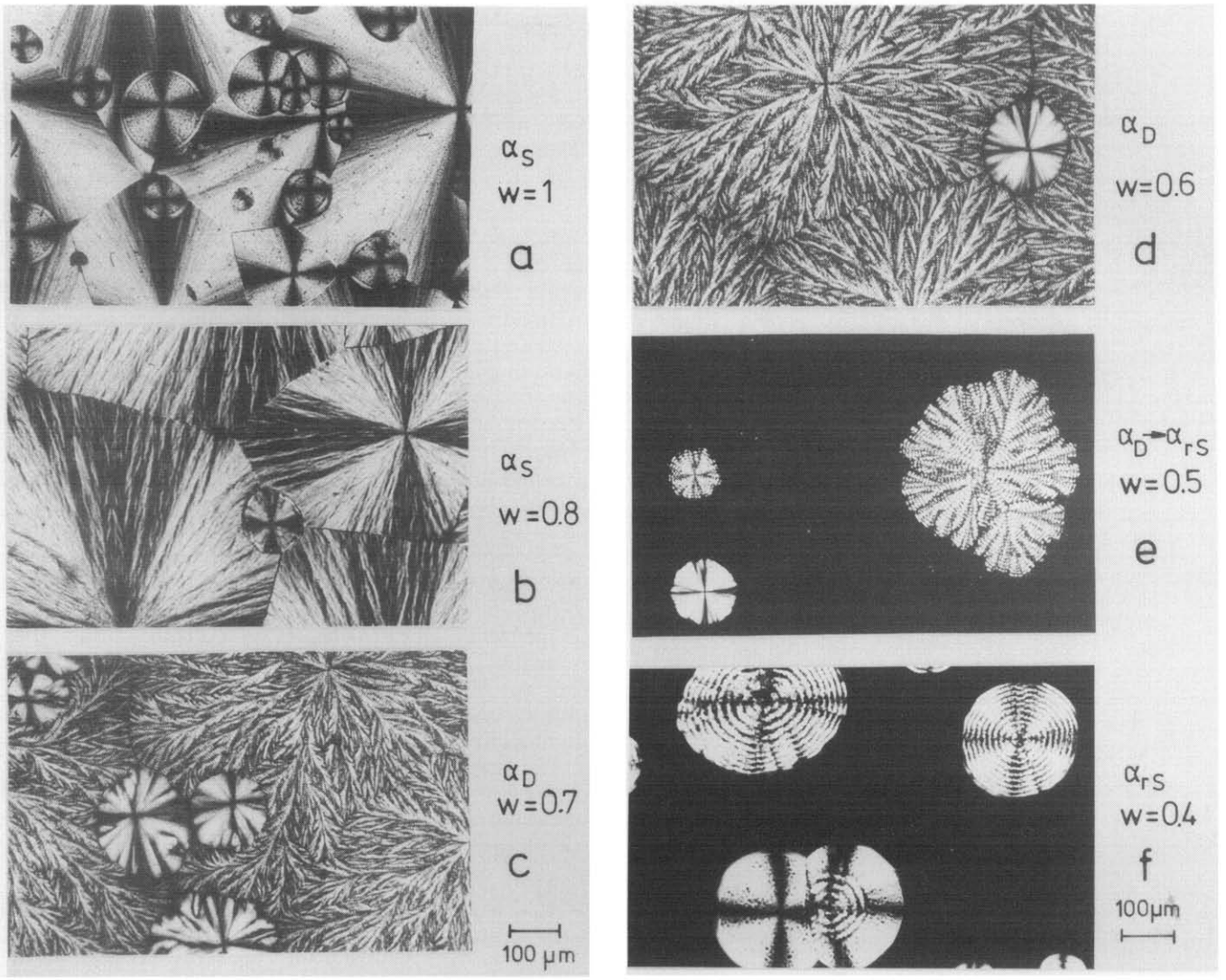

Figure 11 Morphology of the α modification in PVF_2/PSMMA blends with different compositions *w* crystallized for 10 days at 160°C (smaller crystals, internally less structured, of the γ modification are also seen. In (f), the ringed spherulites are α and the unringed γ)

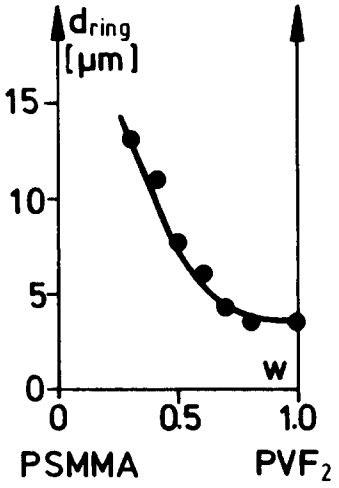

Figure 12 Ring spacing d_{ring} of PVF_2/PSMMA at 160°C

dendritic structure in *Figure 13c* is a 'ghost' of the molten α dendrites. On the contrary, the ring pattern of the spherulites α_{rS} disappears immediately after melting (*Figure 14*).

Crystallization of PVF_2 always involves ejection of the amorphous polymer. When this polymer concentrates somewhere, depletion zones are formed (*Figure 4*) that have less than average of the PVF_2. In dendrites α_D, these zones are incorporated visibly in the crystal. In spherulites α_{rS}, these zones are layers around the crystals, which can be made visible. When partly crystallized blends are crystallized rapidly to completion, in a second step at 120°C, the amorphous matrix is transformed into tiny crystals, except in depletion layers. Such a layer is seen in *Figure 15*, forming a corona around the crystal. These layers were observed around γ and α_{rS} spherulites, but not around α_D dendrites and α_S spherulites.

Scattered over all pictures in *Figures 11*, *13* and *14* are small γ spherulites. They are much less structured. They are never ringed, not even at low *w*. The crystal with a ringed centre in *Figure 11f* is an α_{rS} spherulite that turned γ′ and was afterwards surrounded by a γ spherulite. Such combined spherulites are observed frequently[11]. But also the γ crystals are not always perfect spherulites, void of an internal structure. It is seen in *Figure 11* that their morphology undergoes, with decreasing *w*, a sequence of perfect, imperfect, and again perfect spherulites, parallel to the sequence $\alpha_S \rightarrow \alpha_D \rightarrow \alpha_{rS}$ of the α crystals. *Figure 13c*

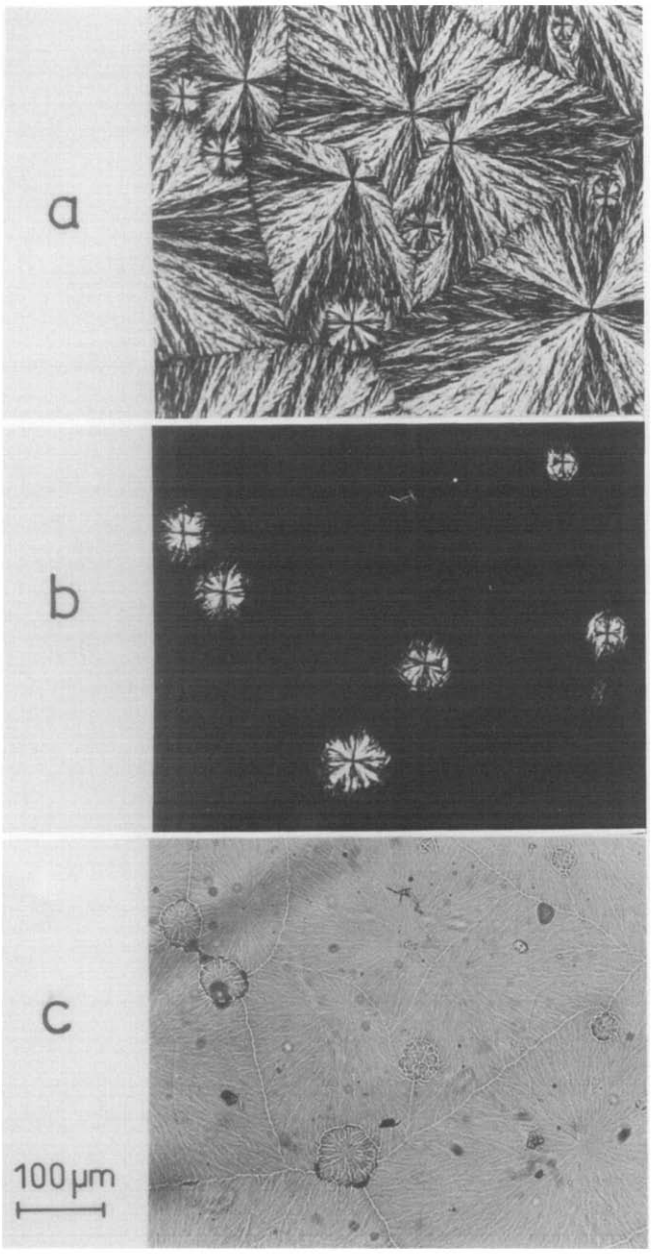

Figure 13 Melting of $PVF_2/PSMMA_{w=0.6}$ crystallized at (a) 150°C, heated to (b) 175°C, where the α modification melted (crossed polars), and to (c) 190°C, where also the γ (and the γ′) modification melted (parallel polars)

reveals that the imperfect γ spherulites are a bit dendritic in character, but without the detailed structure of the α_D dendrites.

Rarely and not reproducibly, γ spherulites produce very irregular structures. In *Figure 16a*, fine branches leave the spherulitic front and penetrate the depletion layer. In *Figure 16b*, feathers grow out of spherulites.

Radial growth rates. Linear radial growth of the crystals is observed for α_D dendrites and α_S spherulites, while γ and α_{rS} spherulites grow non-linearly, in a self-retarding fashion (*Figure 17*). Only the latter two crystals develop a depletion layer, which is evidently the retarding obstacle. Non-linear growth is observed above the transition line indicated in *Figure 10*. The transition dendrite ($\alpha_D \rightarrow \alpha_{rS}$) in *Figure 11e* grew already non-linearly.

The radial growth rate G for α crystals is shown in *Figure 18a*, as a function of temperature (the initial rate, in cases of non-linear growth). The Hoffman–Lauritzen behaviour[25,26] is evident, as it was in *Figure 8b* for the overall crystallization rates. The rates G are higher in the blends with PSMMA, although mobility should be higher in the blends with PMMA, owing to the lower molecular weight (T_g being similar, *Figure 6*). The reason should be that PVF_2 and PSMMA segregate more easily, during crystallization, since they are anyway close to immiscibility (*Figure 5*).

In *Figure 18b*, data of *Figure 18a* were used to construct iso-G curves. Comparison with *Figure 10* reveals that dendrites are observed approximately along the lines for $G = 0.1\ \mu m\ min^{-1}$.

Competition between crystallization and diffusion. The structure of a crystal growing in a blend is sketched in *Figure 19a*, in order to point out where the amorphous polymer can go, if ejected. Branches grow outwards from the centre, more or less radially. Each branch is a stack of lamellae, which is viewed edge-on[29]. The lamellae in a branch are correlated, being connected by tie chains, while different branches are uncorrelated. Four sites are specified in *Figure 19a* for the amorphous polymer. It can go (1) between the lamellae (α_S), (2) between the branches (α_D), (3) into a depletion layer around the crystal (α_{rS}), or (4) anywhere in the still amorphous matrix. The

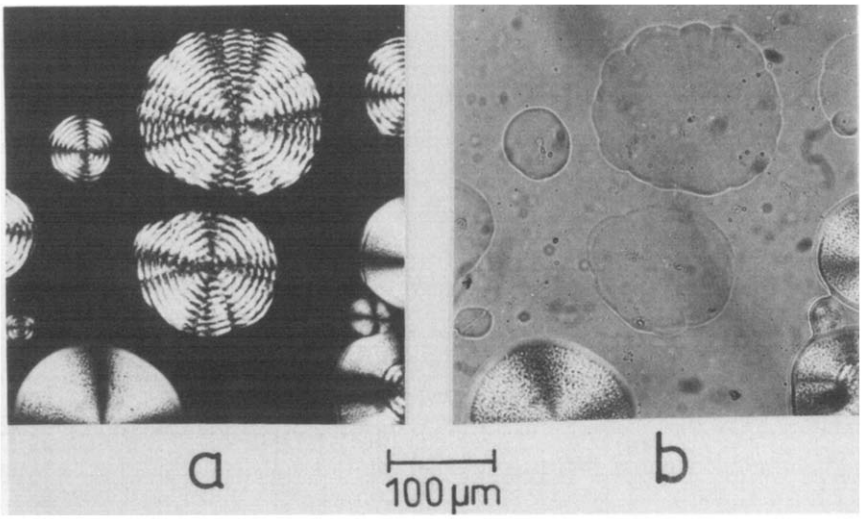

Figure 14 Melting of $PVF_2/PSMMA_{w=0.4}$ crystallized at (a) 160°C (crossed polars) and heated to (b) 180°C, where the α modification melted (parallel polars)

correspondence, $\alpha_S \rightarrow 1$, $\alpha_D \rightarrow 2$ and $\alpha_{rS} \rightarrow 3$, of sites and morphologies is assumed, for the following reasons.

The diffusion distances grow in the order (1)–(4). The morphologies are controlled by the competition of polymer diffusion and crystal growth, as was pointed out by Keith and Padden[22]. They used the ratio D/G of the diffusion coefficient and the radial growth rate, which is a useful parameter for a qualitative discussion of the balance of diffusion and crystallization.

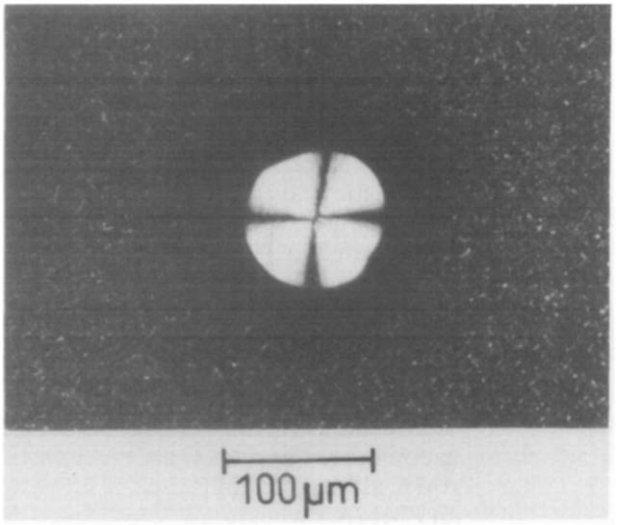

Figure 15 Depletion layer as a dark corona around a γ spherulite crystallized at 164°C. The grey matrix consists of tiny α spherulites crystallized at 120°C

At very low D/G, the amorphous polymer hardly moves and is built in by the growing crystal (site 1). At very high D/G, on the contrary, the amorphous polymer diffuses away from the crystal easily, far into the amorphous matrix (site 4). These extreme situations, (1) and (4), should both lead to spherulites without depletion layers. At intermediate D/G, the amorphous polymer diffuses moderately slowly and remains inside the crystal (site 2), at lower D/G, or just outside of it (site 3), at higher D/G. The former leads to dendrites, the latter to spherulites with a depletion layer.

This amounts to an interpretation of the sequence $\alpha_S \rightarrow \alpha_D \rightarrow \alpha_{rS}$ in terms of the sequence $1 \rightarrow 2 \rightarrow 3$ due to accelerated diffusion of the amorphous polymer, away from the crystallizing PVF_2. There are some comments:

(a) *Spherulites* α_S: If spherulites α_S growing in blends absorb the amorphous polymer between the lamellae (site 1), the interlamellar distance must widen from λ_{PVF_2} to $\lambda = \lambda_{PVF_2}/w$. Indeed, this describes well the X-ray data due to Ullmann and Wendorff[13] shown in *Figure 20*, which were measured for α_S spherulites at a low temperature. Hence, PMMA is indeed incorporated between the lamellae at high crystallization rates.

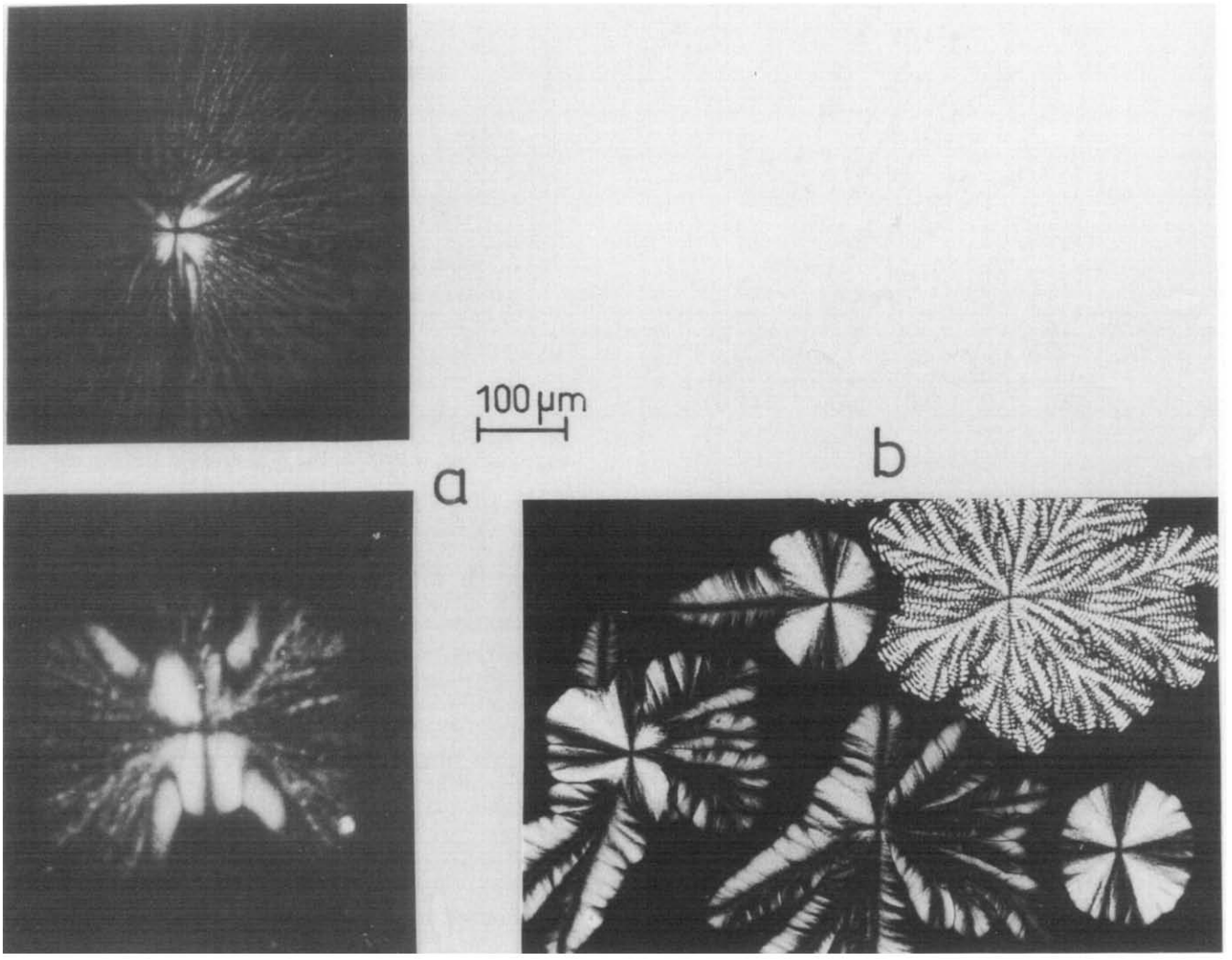

Figure 16 Some γ spherulites in $PVF_2/PMMA_{w=0.5}$ with (a) thin fibrils (164°C) and (b) feathers (155°C). In the upper right-hand corner of (b) is an α_D dendrite

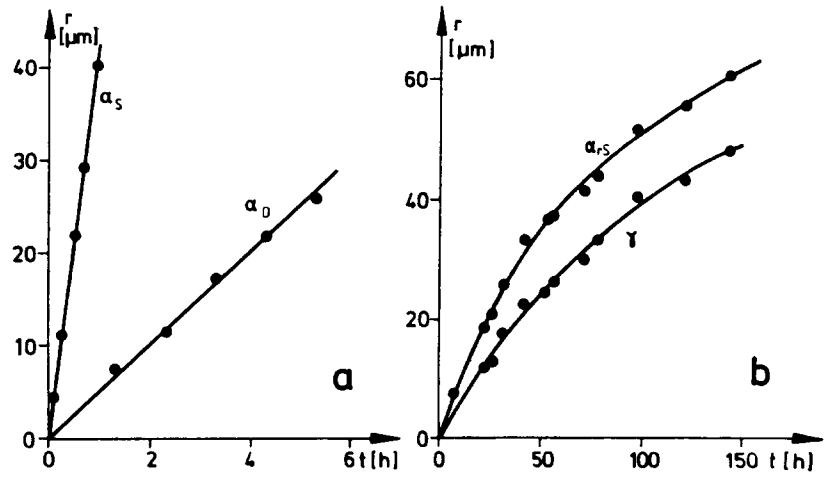

Figure 17 Radial growth of crystals in PVF_2/PSMMA: (a) spherulites α_S ($w=0.7$) and dendrites α_D ($w=0.5$) at 156°C; (b) spherulites γ and α_{rS} ($w=0.5$) at 164°C

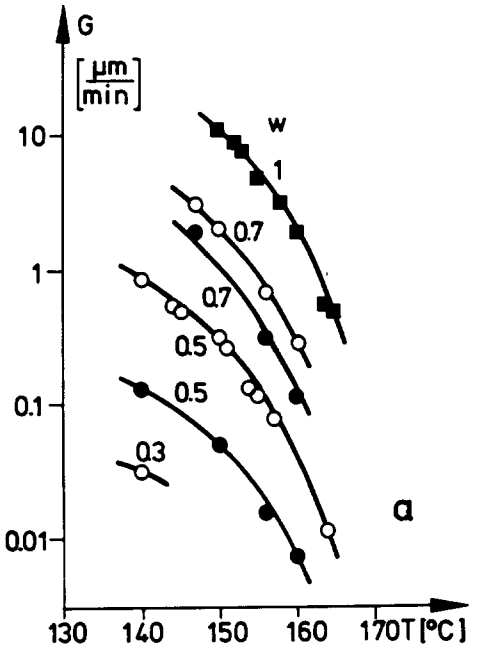

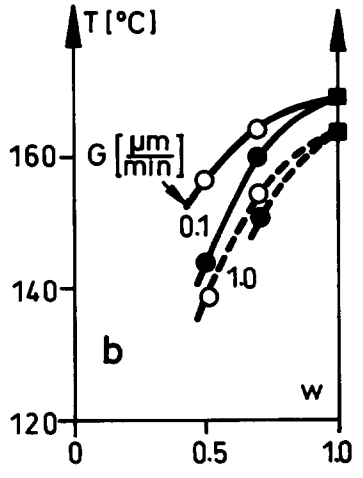

Figure 18 (a) Radial growth rates $G=dr/dt$ of α crystals in PVF_2 (■) and blends PVF_2/PMMA (●) and PVF_2/PSMMA (○). (b) Curves of a constant rate G in a phase diagram such as *Figure 10*

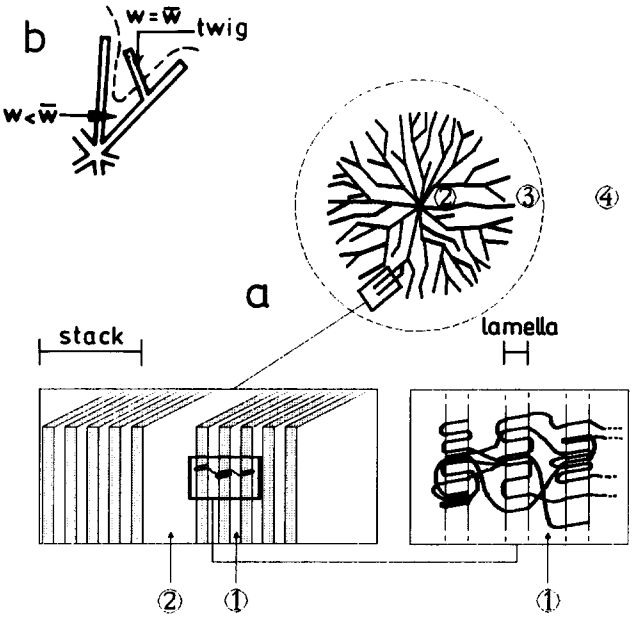

Figure 19 (a) Schematic picture of a crystal in a blend with four sites where the amorphous polymer can concentrate. (b) Growth of a twig from a branch through a depletion layer $w<\bar{w}$

(b) *Dendrites* α_D: A depletion layer that does not move fast enough away from the advancing crystal provokes instabilities. Some branches will cut through the layer and keep growing (*Figure 4b*), and the layer will split up into radial depletion zones between the branches (site 2). Twigs grow into these zones, by the same mechanism as the branches (*Figure 19b*). The depletion $w<\bar{w}$ is strongest along the branches. To cut through this zone, the twigs must grow at large angles to the branch, not parallel to it, as they would in a spherulite. In summary, dendritic growth is crystallization through depletion zones.

(c) *Spherulites* α_{rS}; The transition $\alpha_D \rightarrow \alpha_{rS}$ to the spherulites α_{rS} occurs when the amorphous polymer flows faster out of, and the PVF_2 faster into, the radial depletion zones (site 2). Crystallization is then faster in these zones, and the amorphous polymer leaves the crystal, forming a depletion layer around it (site 3).

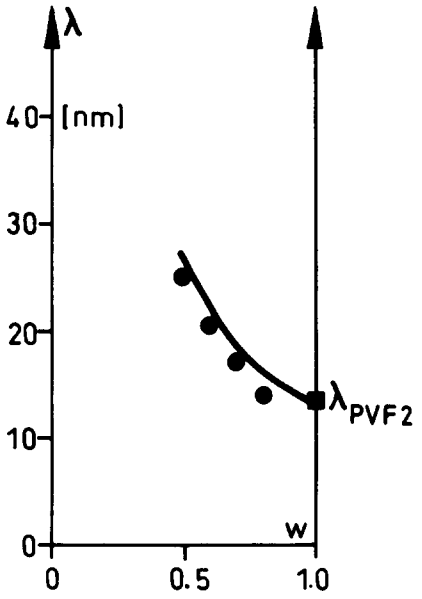

Figure 20 Long period λ of the lamellar stacks in PVF_2/PMMA crystallized at 140°C (data from ref. 13); the curve is given by $\lambda = \lambda_{PVF_2}/w$

(d) *Parameter D/G*: The sequences $\alpha_S \rightarrow \alpha_D \rightarrow \alpha_{rS}$ and $1 \rightarrow 2 \rightarrow 3$, in the view adopted by Keith and Padden[22], are consequences of a growing ratio D/G. This parameter is useful, but not perfect. It contains the blend concentration w only implicitly. Secondly, it is not specified which diffusion coefficient is crucial, that of PVF_2, that of the amorphous polymer (which is Keith and Padden's opinion[22]), or the interdiffusion coefficient (which is other authors' suggestion[30]). A third problem concerns *Figure 10*. In the phase diagrams, D grows, according to the Williams–Landel–Ferry (WLF) model[31], in the direction northeast (normal to T_g, *Figure 6*), and G grows in the direction southeast (normal to the iso-G curves, *Figure 18b*). Therefore, D/G should increase more or less in the direction north, i.e. with increasing temperature, and this should also be the direction of the sequence $\alpha_S \rightarrow \alpha_D \rightarrow \alpha_{rS}$ of morphologies in *Figure 10*. But this sequence points, in *Figure 10*, clearly in the direction northwest. Dendrites α_D are observed in the range of practically constant growth rate, $G = 0.1\ \mu m\ min^{-1}$ (*Figures 10* and *18b*). A more detailed understanding is required.

Nonetheless, if the range for dendrites α_D in *Figure 10* is roughly a range of constant D/G, it should be shifted if D is changed by changing the chain length of the amorphous polymer. This was proved with blends $PVF_2/PMMA_{w=0.5}$ at 150°C. The blend with the PMMA used throughout this study forms dendrites, while a blend with an oligomeric PMMA ($M_w = 6 \times 10^3$) yielded spherulites α_{rS}, and a blend with a very long-chain PMMA ($M_w = 450 \times 10^3$) gave spherulites α_S. Diffusion is faster in the former case and slower in the latter. The morphology responds as expected, for a higher and a lower D/G, respectively.

Blends with PMA

PVF_2/PMA blends have much lower glass transition temperatures than the blends considered so far (*Figure 6*). Diffusion and crystallization are, therefore, faster, so that even blends with low PVF_2 contents w could be investigated. The radial growth rates G are shown in *Figure 21*. PVF_2 was expected to crystallize in these blends under conditions of fast diffusion, compared to the crystallization.

The distribution of morphologies in *Figure 22a* agrees with this assumption. The blends form mostly ringed spherulites α_{rS}. The ring spacings d_{ring} are shown in *Figure 22b* and morphologies in *Figure 23*. No dendrites were observed. The spherulites α_{rS} grow linearly, unlike their counterparts in the last section (*Figure 17b*), and they hardly exhibit depletion layers. All this corresponds to conditions of fast diffusion. Evidently, PMA diffuses easily far away from the crystals (site 4, *Figure 19a*).

Of special interest is crystallization at very low w, when PVF_2 is strongly diluted by PMA. Blends with low w should be the realm of loose structures, like dendrites. Indeed, the crystals in *Figure 24* look a bit like dendrites. However, these are embryos (sometimes called axialites[22,32]), as are frequently observed in the early stages of spherulitic growth. The spherulites α_{rS} in *Figure 23* had similar (small) early stages that turned into spherulites after the first ring. The crystals in *Figure 24*

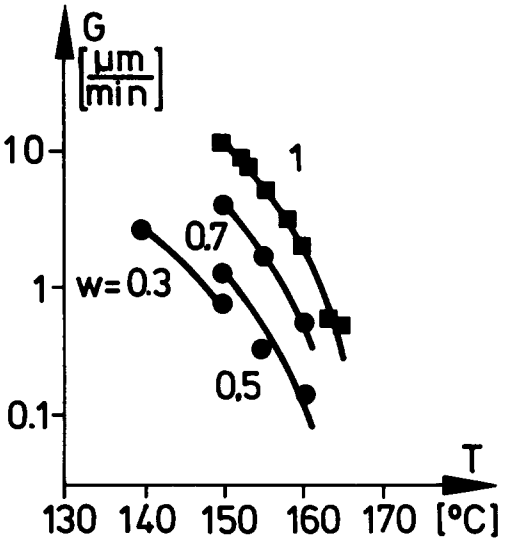

Figure 21 Radial growth rates G of α crystals in PVF_2/PMA

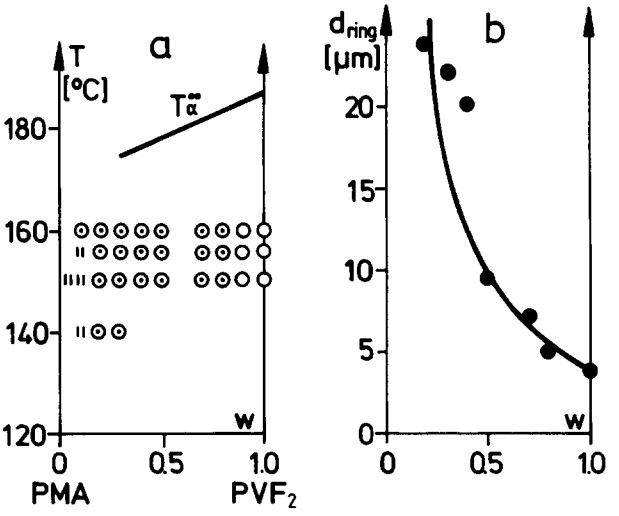

Figure 22 Types of morphology of the α modification in PVF_2/PMA: (○) α_S, (⊙) α_{rS}, (‖) embryos. (b) Ring spacing d_{ring} at 156°C

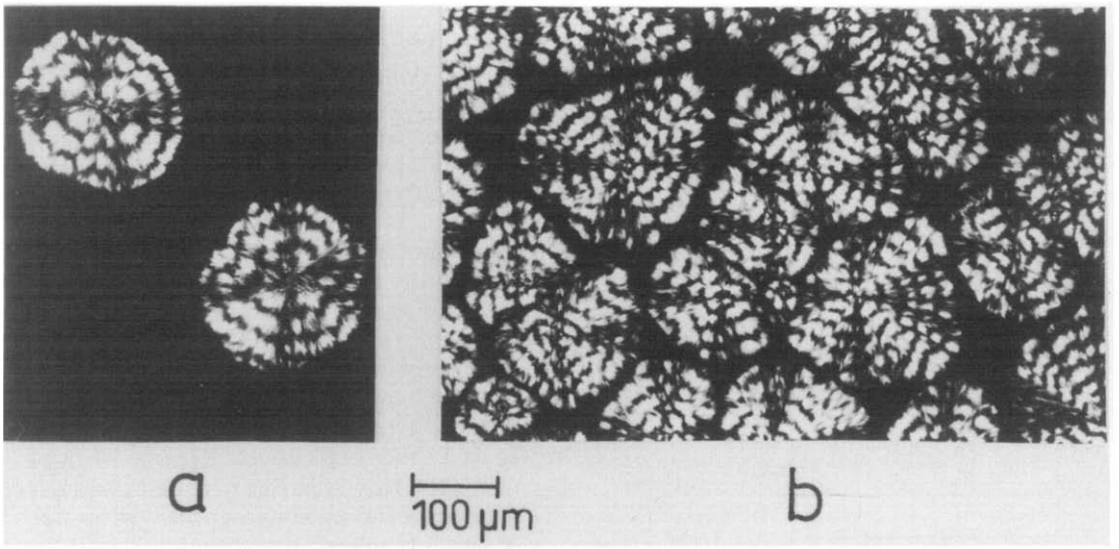

Figure 23 Ringed spherulites α_{rS} in $PVF_2/PMA_{w=0.2}$ crystallized at (a) 160°C and (b) 156°C

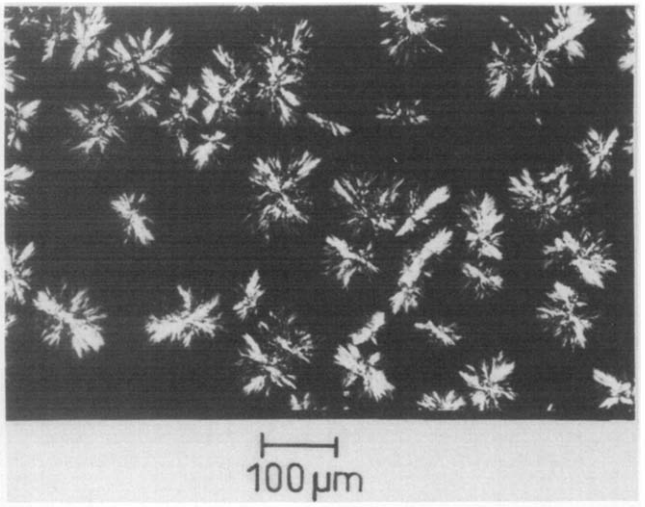

Figure 24 Embryos in $PVF_2/PMA_{w=0.5}$ crystallized at 150°C

are thus not in any way special, they are merely unusually large embryos.

In conclusion, the blends PVF_2/PMA complete the picture, by adding the site 4, for the amorphous polymer, to the sites 1–3 already observed in the blends PVF_2/PMMA and PVF_2/PSMMA.

CONCLUSIONS

The fibrillar texture of the α spherulites in pure PVF_2 (*Figure 2*) seems to indicate a propensity of the α modification towards irregular structures, for which the ring pattern is a second indication. Neither feature is found in γ spherulites of pure PVF_2. The conclusion should be that blending PVF_2 with an amorphous polymer merely exaggerates intrinsic properties of the α modification. Yet, dilution of the PVF_2 does not necessarily change much. In the blends PVF_2/PMA, where diffusion and crystallization are not much slower than in pure PVF_2, only the ring pattern in the α crystals is changed (*Figure 23*). Dendrites do not appear.

The condition for the spectacular cauliflower structures of the α_D dendrites is evidently not simply dilution. A gradient of concentration at the crystallizing front is necessary. Only if radial depletion zones are built up, by an ejected amorphous polymer that diffuses relatively slowly, does the α modification produce isolated radial branches and twigs on them, instead of a dense array of radial branches. *The dendrites are evidently the product of crystal growth in the direction of the concentration gradients* (*Figure 19*).

In computer simulations, loosely structured dendrites can be produced by diffusion-controlled crystallization[20], which should occur far below the melting point (below 120°C, *Figure 8b*) or at very high dilution of the PVF_2. But dendrites are observed in *Figure 10* at moderate undercoolings and at high concentrations of PVF_2. The former can probably be reproduced in simulations after incorporation of an activation energy for nucleation. More surprising is the latter phenomenon, the formation of dendrites at high concentrations of PVF_2. To provoke the growth of twigs, there must be pronounced depletion zones along the branches, as was indicated in *Figure 19b*. But such pronounced depletion is unexpected in blends of a high PVF_2 concentration. This point needs further investigation.

Dendritic structures in blends with low contents of an amorphous polymer are of interest, because these morphologies are co-continuous. As in amorphous blends with a co-continuous phase structure[33], neither of the phases is dispersed, in finite domains, inside the matrix of the other phase. The crystalline as well as the amorphous phase build up a phase network (or an 'infinite cluster'). As in amorphous blends, this may lead to unusual mechanical properties, if the amorphous polymer is an elastomer and the crystals are small. The elastomer could act as an impact modifier. According to the above, however, a faster crystallizing polymer than PVF_2 would be needed, to produce dendrites in such blends.

ACKNOWLEDGEMENT

Financial support from the Bundesminister für Wirtschaft through the Arbeitgemeinschaft Industrieller Forschungsvereinigungen (AIF) is gratefully acknowledged.

REFERENCES

1 Lovinger, A. J. *Polymer* 1980, **21**, 1317; *J. Polym. Sci., Polym. Phys. Edn.* 1980, **18**, 793; *Macromolecules* 1981, **14**, 322
2 Mancarella, C. and Martuscelli, E. *Polymer* 1977, **18**, 1240
3 Welch, G. J. and Miller, R. L. *J. Polym. Sci., Polym. Phys. Edn.* 1976, **14**, 1683
4 Osaki, S. and Ishida, Y. *J. Polym. Sci., Polym. Phys. Edn.* 1975, **13**, 1071
5 Nasagawa, N. and Ishida, Y. *J. Polym. Sci., Polym. Phys. Edn.* 1973, **11**, 2153
6 Prest, W. M. and Luca, D. J. *J. Appl. Phys.* 1975, **46**, 4136; 1978, **49**, 5042
7 Marand, H. L., Stein, R. S. and Stack, G. M. *J. Polym. Sci., Polym. Phys. Edn.* 1988, **26**, 1361; 1989, **27**, 1089
8 Lovinger, A., Davis, D. D., Cais, R. E. and Kometani, J. M. *Polymer* 1987, **28**, 617
9 Nakamura, S., Sasaki, T., Funamoto, J. and Matsuzaki, K. *Makromol. Chem.* 1975, **176**, 3471
10 Nandi, A. K. and Mandelkern, L. *J. Polym. Sci., Polym. Phys. Edn.* 1991, **29**, 1287
11 Morra, B. S. and Stein, R. S. *J. Polym. Sci., Polym. Phys. Edn.* 1982, **20**, 2243, 2261; *Polym. Eng. Sci.* 1984, **24**, 311
12 Wang, T. T. and Nishi, T. *Macromolecules* 1975, **8**, 909; 1977, **10**, 421
13 Ullmann, W. and Wendorff, J. H. *Compos. Sci. Technol.* 1985, **23**, 97
14 Hahn, B., Wendorff, J. H. and Yoon, D. Y. *Macromolecules* 1985, **18**, 718
15 Leonard, C., Halary, J. L. and Monnerie, L. *Macromolecules* 1988, **21**, 2988
16 Jo, W. H., Yoon, J. T. and Lee, S. C. *Polym. J.* 1991, **23**, 1243
17 Wahrmund, D. C., Bernstein, R. E., Barlow, J. W. and Paul, D. R. *Polym. Eng. Sci.* 1978, **18**, 677, 1225
18 Bernstein, R. E., Cruz, C. A., Paul, D. R. and Barlow, J. W. *Macromolecules* 1977, **10**, 681
19 Takahashi, Y. and Tadokoro, H. *Ferroelectrics* 1984, **57**, 187
20 Witten, T. A. and Sander, L. M. *Phys. Rev. Lett.* 1981, **47**, 1400; *Phys. Rev. (B)* 1983, **27**, 5686
21 Langer, J. S. and Müller-Krumbhaar, H. *Acta Metall.* 1978, **26**, 1681, 1689, 1697
22 Keith, H. D. and Padden, F. J. *J. Appl. Phys.* 1963, **34**, 2409; 1964, **35**, 1270, 1286; *Polymer* 1986, **27**, 1463; *J. Polym. Sci., Polym. Phys. Edn.* 1987, **25**, 229, 2265, 2371d
23 Wendorff, J. H. *J. Polym. Sci., Polym. Lett. Edn.* 1980, **18**, 439
24 Hoffman, J. D. and Weeks, J. J. *J. Res. NBS (A)* 1961, **66**, 13
25 Hoffman, J. D. *SPE Trans.* 1964, **4**, 315
26 Hoffman, J. D. *Polymer* 1982, **23**, 656; 1983, **24**, 3
27 Keith, H. D. and Padden, F. J. *J. Polym. Sci.* 1959, **39**, 101, 123
28 Keller, A. *J. Polym. Sci.* 1959, **39**, 151
29 Bassett, D. C. and Hodge, A. M. *Proc. R. Soc. Lond. (A)* 1981, **377**, 61
30 Alfonso, G. C. and Russell, T. P. *Macromolecules* 1986, **19**, 1143
31 Williams, M. L., Landel, R. F. and Ferry, J. D. *J. Am. Chem. Soc.* 1955, **77**, 3701
32 Bassett, D. C., Keller, A. and Mitsuhashi, S. *J. Polym. Sci. (A)* 1963, **1**, 763
33 Andradi, L. N. and Hellmann, G. P. *Polymer* 1993, **34**, 925